

# MD/GE - Molecular dynamics simulation and lattice energy of argon

Protocol for the PC 2 lab course by  
**Vincent Kümmerle & Elvis Gnaglo & Julian Brügger**

University of Stuttgart

authors: Vincent Kümmerle, 3712667  
st187541@stud.uni-stuttgart.de

Elvis Gnaglo, 3710504  
st189318@stud.uni-stuttgart.de

Julian Brügger,  
st190010@stud.uni-stuttgart.de

group number: A05

date of experiment: 10.12.2025

supervisor: Xiangyin Tan

submission date: December 16, 2025

**Abstract:**

# Contents

<b>1 Theory</b>	<b>1</b>
<b>2 Procedure</b>	<b>3</b>
2.1 Molecular Dynamics Simulations . . . . .	3
2.2 Lattice Energy of Argon . . . . .	3
<b>3 Results</b>	<b>5</b>
<b>4 Analysis</b>	<b>7</b>
4.1 Molecular Dynamics Simulations . . . . .	7
4.1.1 Isochor simulations . . . . .	7
4.1.2 Isobaric simulations . . . . .	9
4.2 Lattice Energy of Argon . . . . .	11
<b>5 Error Discussion</b>	<b>14</b>
<b>6 Conclusion</b>	<b>14</b>
<b>7 References</b>	<b>14</b>

## 1 Theory

Molecular dynamics simulations (MDS) are used to visualize spatial movements of atoms and molecules. For that a numerical algorithm can determine the positions  $r_i$  and momentums  $p_i$  for each particle  $i$ .<sup>[1]</sup> A proven algorithm is the Velocity-Verlet algorithm, which assigns each particle a random starting position and velocity at first before calculating the new positions and velocities a small time step later. That is achieved by calculating the new accelerations using the provided potential, e.g. lennard-Jones potential. So for the computation of particle trajectories in MDS the equation of motion is integrated and then the forces induced by potentials are calculated. To approximate the intermolecular interactions between particles, the Lennard-Jones potential (LJ-potential)  $V_{ij}$  with equation 1 is used.<sup>[1]</sup>

$$V(r_{ij}) = 4\epsilon_0 \left[ \left( \frac{\sigma_0}{r_{ij}} \right)^{12} - \left( \frac{\sigma_0}{r_{ij}} \right)^6 \right], \quad (1)$$

$\sigma_0$  describes the minimum distance,  $r_{ij}$  the distance between particle  $i$  and  $j$  and  $\epsilon_0$  the depth of the potential well at the equilibrium distance  $r_e$ , which can be seen in figure 1. The positive part with a twelfth power-term characterizes the repulsive interactions to the nearest neighbours, whereas the negative part with a sixth power-term characterizes the attractive electrostatic interactions.<sup>[1]</sup>

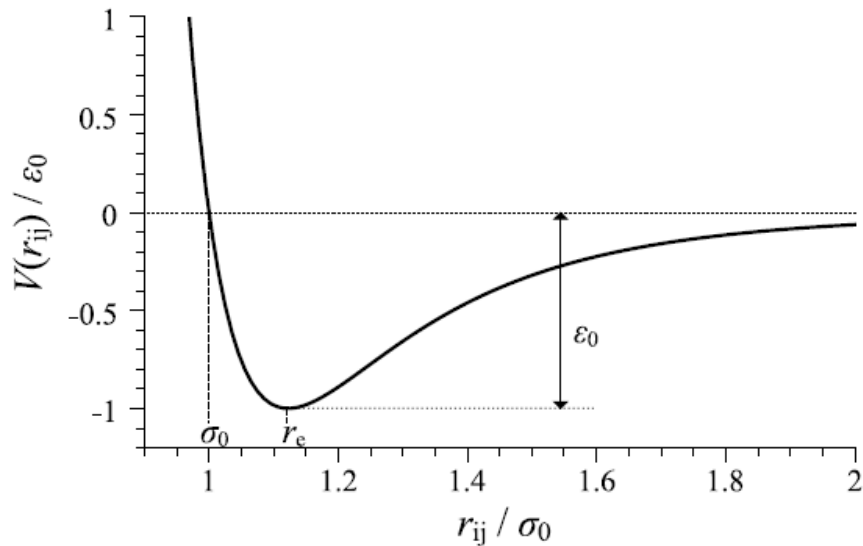


Figure 1: Potential curve of a Lennard-Jones potential  $V_{ij}$  depending on the particle distance  $r_{ij}$ .<sup>[1]</sup>

In MDS reduced properties are used to describe thermodynamical states by defining units and setting the value to 1.0 for shorter calculation times. When using the LJ-potential the fundamental units  $\epsilon_0$ ,  $\sigma_0$  and the mass  $m$  are set to 1.0. In the experiment the reduced units of pressure  $p^*$  and temperature  $T^*$  are used, which can be calculated with equation 2 and 3.

$$T^* = \frac{k_B T}{\varepsilon_0} \quad (2)$$

$$p^* = \frac{p \sigma_0^3}{\varepsilon_0} \quad (3)$$

In an isolated system, where the gaseous and solid phase are in equilibrium and the volume of the gas is much bigger than the volume of the liquid, the Clausius-Clapeyron equation 4 can be used to describe the dependence of the sublimation pressure  $p$  on the temperature  $T$ .

$$\ln p = -\frac{\Delta H_{\text{sub}}}{RT} + C \quad (4)$$

The enthalpy of sublimation  $\Delta H_{\text{sub}}$  can be determined by plotting  $\ln p$  against  $1/T$ . Argon behaves like an ideal gas at 70 K and the internal energy  $\Delta U$  during a phase transition from solid to gaseous is the difference of the corresponding internal energies. Because the translational energy of gaseous argon corresponds to the kinetic theory of gases, the total internal energy of the solid  $U_s$  can be calculated with equation 6.

$$U_s = \frac{5}{2}RT - \Delta H \quad (5)$$

$U_s$  consists of two parts, which are described in equation 5.<sup>[1]</sup>

$$\Delta U_s = U_{\text{lattice}} + U_{\text{vib}} \quad (6)$$

The first part corresponds with the potential energy of argon atoms at rest on their lattice planes, whereas the second part is the vibrational energy of the atoms. For the calculation of  $U_{\text{vib}}$ , Debyes theory is used, which states that the crystal is composed as independent vibrating lattice atoms with varying frequencies. For that the equation 7 shows the connection between the vibrational energy and the Debye-temperature  $\Theta_D$ .

$$U_{\text{vib}} = \frac{9}{8}R\Theta_D + 3RTD \left( \frac{\Theta_D}{T} \right) \quad (7)$$

To calculate the theoretical value of the lattice energy, equation 8 can be used, which is derived from the pair potentials  $V_{ij}(r_{ij})$  in the LJ-potential equation 1.

$$U_{\text{lattice}}(s) = 2N_A\varepsilon_0 \left[ 12.132 \left( \frac{\sigma_0}{a} \right)^{12} - 14.454 \left( \frac{\sigma_0}{a} \right)^6 \right] \quad (8)$$

$N_A$  is Avogadro's constant and  $a$  the distance between atoms.

## 2 Procedure

### 2.1 Molecular Dynamics Simulations

The computational work consisted of three sequential simulation tasks carried out using pre-written Python programs. In the first task, the behavior of argon particles was investigated under conditions of increasing temperature at constant pressure. The simulation focused on visualizing particle motion and the associated expansion of the system volume. To achieve this, the number of cooling steps was gradually increased, followed by an adjustment of the interaction potential depth in order to observe its influence on the system dynamics. In the second task, the sublimation behavior of argon was studied by analyzing the relationship between temperature and pressure at constant volume. Two simulations were performed with different numerical resolutions. Initially, the system was simulated using 100 cycles with 1000 steps. In a subsequent run, the parameters were increased to 200 cycles and 4000 steps. The resulting pressure-temperature dependence obtained from the simulations was then compared with the experimental measurements. The third task addressed the temperature dependence of the system volume. For this purpose, three simulations with progressively increased numerical accuracy were carried out. The first simulation employed 50 cooling cycles with 100 cooling steps, followed by 10 cycles and 100 steps. In the second simulation, the cooling cycles were increased to 100, the cooling steps to 1000, and the number of cycles to 100. In the final simulation, the number of steps was further increased to 1000. The results of these simulations were compared in order to analyze phase transitions and to determine the melting and boiling points of argon.

### 2.2 Lattice Energy of Argon

The experimental setup was preassembled prior to the start of the measurements as shown in figure 2.



Figure 2: Scheme of the measuring apparatus.<sup>[1]</sup>

The experiment began with the removal of residual gases from the system. This was achieved by flushing the apparatus with nitrogen gas followed by evacuation. Subsequently, the pressure was monitored for two minutes to verify the absence of leaks. After confirming system integrity, the argon chamber was adjusted to a pressure of approximately 250 mbar and cooled to 63.9 K, leading to a pressure decrease to about 20 mbar. At this stage, the measured pressure served as an indicator of gas purity, as significantly higher pressures would indicate contamination by other gases. Once a pressure of approximately 15.4 mbar was reached, the nitrogen chamber was filled to the required level and likewise cooled to 63.9 K. After all pressures stabilized, the valves were closed, the Dewar vessel was sealed, and the vacuum pump was activated. Pumping nitrogen gas from the Dewar further reduced the system temperature. Under these conditions, the pressure in the argon chamber was approximately 0.154 bar, while the nitrogen chamber reached about 0.0144 bar. After maintaining constant pressure for an additional five minutes, the pump was switched off and the system was allowed to warm up. During the warming phase, the pressures in both chambers were recorded at intervals of 30 seconds. This data was later compared with the results from the second simulation task and used for the determination of the lattice energy of argon.

### 3 Results

The determination of the sublimation energy of argon requires the calculation of the temperature. This can be done by using the Henning-Otto-Equation (9), which uses the measured pressure of nitrogen after conversion into torr, which are shown in Table 1, to calculate the temperature of the system.

$$\log(p/\text{Torr}) = 7.781845 - \frac{341.619 \text{ K}}{\text{T}} - 0.0062649 \frac{\text{T}}{\text{K}} \quad (9)$$

Table 1: Listed are the measured and transformed pressures of argon and nitrogen as well as the calculated temperature of the system.

$t$ [s]	$p_{\text{Ar}}$ [bar]	$p_{\text{N}_2}$ [bar]	$p_{\text{Ar}}$ [Torr]	$T$ [K]
0	0.1540	1.4440	11.5510	63.8906
30	0.1760	1.5000	13.2011	64.1048
60	0.1760	1.4960	13.2011	64.0897
90	0.1810	1.5320	13.5761	64.2243
120	0.2220	1.6960	16.6514	64.8069
150	0.2460	1.8340	18.4515	65.2629
180	0.2680	1.9390	20.1017	65.5917
210	0.2870	2.0390	21.5268	65.8918
240	0.3060	2.1560	22.9519	66.2282
270	0.3330	2.2830	24.9771	66.5773
300	0.3460	2.4130	25.9521	66.9189
330	0.3850	2.5490	28.8774	67.2609
360	0.4170	2.6940	31.2776	67.6098
390	0.4480	2.8440	33.6028	67.9554
420	0.4810	2.9960	36.0780	68.2912
450	0.5190	3.1710	38.9282	68.6614
480	0.5650	3.3370	42.3785	68.9980
510	0.6040	3.5220	45.3037	69.3578
540	0.6480	3.7060	48.6040	69.7012
570	0.6920	3.8900	51.9043	70.0315
600	0.7430	4.0910	55.7296	70.3785
630	0.7980	4.2930	59.8549	70.7141

660	0.8480	4.4890	63.6053	71.0281
690	0.8940	4.6940	67.0555	71.3452
720	0.9570	4.9070	71.7809	71.6635
750	1.0140	5.1370	76.0563	71.9954
780	1.0770	5.3570	80.7817	72.3022
810	1.1460	5.6200	85.9571	72.6564
840	1.2130	5.8230	90.9825	72.9211
870	1.2830	6.0500	96.2330	73.2088
900	1.3550	6.2970	101.6334	73.5125
930	1.4130	6.5250	105.9838	73.7849
960	1.4970	6.7740	112.2843	74.0741
990	1.5700	7.0310	117.7597	74.3642
1020	1.6530	7.2790	123.9852	74.6365
1050	1.7270	7.5300	129.5357	74.9050
1080	1.8130	7.7830	135.9862	75.1687
1110	1.8970	8.0410	142.2868	75.4311
1140	1.9070	8.3000	143.0368	75.6881
1170	2.0600	8.5520	154.5128	75.9324
1200	2.1470	8.8050	161.0383	76.1722
1230	2.2410	9.0590	168.0889	76.4078
1260	2.3400	9.3610	175.5145	76.6814
1290	2.4320	9.6220	182.4151	76.9126
1320	2.5220	9.8950	189.1656	77.1494
1350	2.6150	10.1790	196.1412	77.3906

## 4 Analysis

### 4.1 Molecular Dynamics Simulations

#### 4.1.1 Isochor simulations

The temperatures and pressures calculated in the simulations of the second task are reported in reduced units and shown in Figure 3.



Figure 3: The reduced temperature is plotted against the reduced pressure for 100 cycles and 1000 steps (T2p1, blue) and for 200 cycles and 4000 steps (T2p2, red).

Both simulations show a very low incline before the sublimation, a steep slope while the sublimation and a transition into a linear increase of the pressure after the sublimation has ended. By increasing the number of iteration steps and the number of iterations per temperature from the first simulation T2p1 to the second T2p2, the begin of the big increase in pressure shifts to a higher temperature, while both curves lead to the same value of pressure, from which on they show the same linear increase. To compare the simulation results to the experimental results, the values of the reduced temperature and pressure are converted from reduced units into Kelvin and Pascal by rearranging equations 2 and 3 to the temperature and pressure:

$$T = \frac{T^* \varepsilon_0}{k_B} \quad (10)$$

$$p = \frac{p^* \varepsilon_0}{\sigma_0^3} \quad (11)$$

For Argon the best values, which were determined from other properties of the gas, are  $\varepsilon_0 = 1.643 \times 10^{-21}$  J and  $\sigma_0 = 3.41 \times 10^{-10}$  m.<sup>[2]</sup> By inserting these values in equation 10 and 11, the values of  $T$  and  $p$  are calculated and then plotted with the experimental data from table 1, which is shown in Figure 4.



Figure 4: The converted temperature is plotted against the converted pressure from the short simulation (T2p1, blue), long simulation (T2p2, red) and the experimental values (green).

Figure 4 shows that the sublimation curve of the longer simulation with more iteration steps and cycles is closer to the experimental data than the shorter simulation. But still, the experimental sublimation curve is located around 10K higher, which can be caused by the approximation of the interactions, which are made in the Lennard-Jones potential. Furthermore, it can be concluded that a higher computation time with more iteration steps and cycles in the Velocity-Verlet algorithm would be necessary to fit the simulation values to the experimental values.

#### 4.1.2 Isobaric simulations

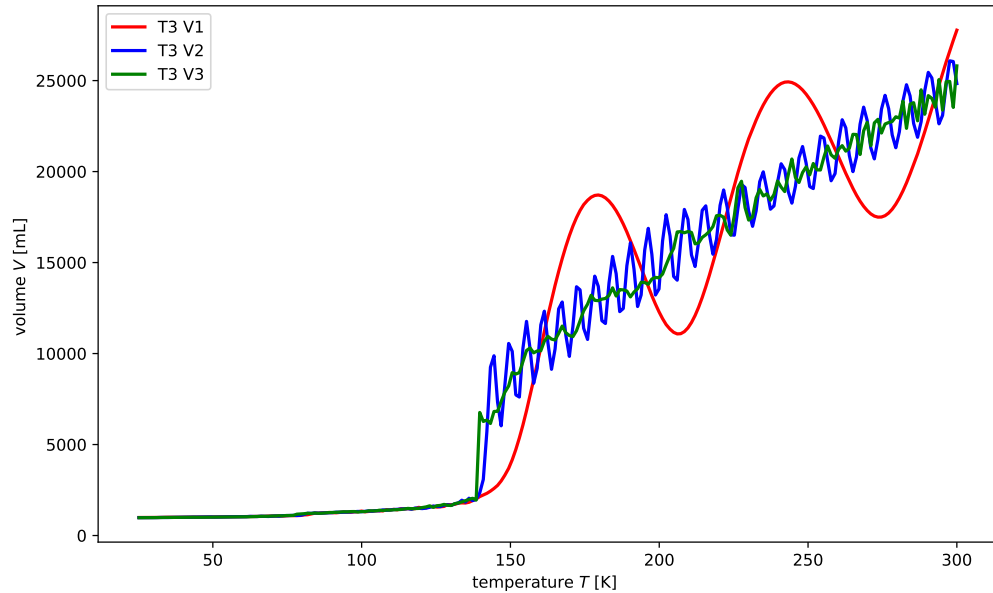


Figure 5: The volume plotted over the temperature for the three simulations.

Plot T3V1 corresponds to the simulation performed with 50 cooling cycles, 100 cooling steps, 10 cycles, and 100 steps. Plot T3V2 represents the simulation using 100 cooling cycles, 1000 cooling steps, 100 cycles, and 100 steps, while plot T3V3 shows the simulation with identical parameters to the second case but with the number of steps increased to 1000. A comparison of the three simulations reveals a clear reduction in oscillatory behavior as the number of cycles and steps increases. Simulations with a lower numerical resolution do not sufficiently sample the available microstates, which results in pronounced oscillations between gas-like and liquid-like configurations. By increasing the number of steps, these fluctuations are significantly reduced, leading to a smoother volume–temperature curve and minimal background noise, as observed in plot ???. Higher step and cycle counts also allow the phase transitions to be identified more distinctly. This is evident from the abrupt increase in volume in plot T3V3, which is much more pronounced than in plots T3V1 and T3V2. To determine the melting and boiling points, the regions of rapid volume increase were analyzed in greater detail. These characteristic changes are highlighted in figures and.



Figure 6: The volume plotted over the temperature for the three simulations between 70 K and 90 K.

In figure 6, the increase in volume is associated with the onset of melting. For the simulation T3V3, this transition begins at approximately 77 K, whereas for T3V2 and T3V1 it occurs at around 79 K, although the melting point in T3V1 is less clearly defined due to stronger variation in the volume increase. In all cases, the steep rise in volume transitions back into the approximately linear behavior observed at lower temperatures once a temperature of about 82 K is reached. The melting temperatures obtained from the simulations deviate from the literature value for argon, which is approximately 84 K<sup>[3]</sup>. This discrepancy can be attributed to the simplified nature of the simulation model. Since not all intermolecular interactions and many-body effects are fully represented, the resulting potential landscape is effectively altered, leading to an underestimation of the melting point.



Figure 7: The volume plotted over the temperature for the three simulations between 110 K and 150 K.

When examining figure 7, an increase in volume is observed for the simulations T3V2 and T3V3, while no comparable feature is present in T3V1. This behavior arises from the increased number of cycles and steps used in T3V2 and T3V3, which results in improved sampling of the phase space and, consequently, a more accurate representation of the phase transition. This interpretation is further supported by the fact that the volume increase in T3V3 is sharper than in T3V2. The observed incline occurs at approximately 137 K, which deviates significantly from the literature boiling point of argon at 87 K. As with the melting point, this discrepancy can be attributed to simplifications and approximations inherent to the simulation model. In this case, the simulated boiling point exceeds the experimental value, suggesting that the interparticle interactions may be overestimated, thereby stabilizing the condensed phase and shifting the boiling transition to higher temperatures.

## 4.2 Lattice Energy of Argon

In order to calculate the lattice energy of argon, the measured sublimation enthalpy must first be calculated. The sublimation enthalpy can be determined by plotting the natural logarithm of the pressure of argon in bar from table 1 against  $\frac{1}{T}$ . Figure 8 shows the the plotted data.

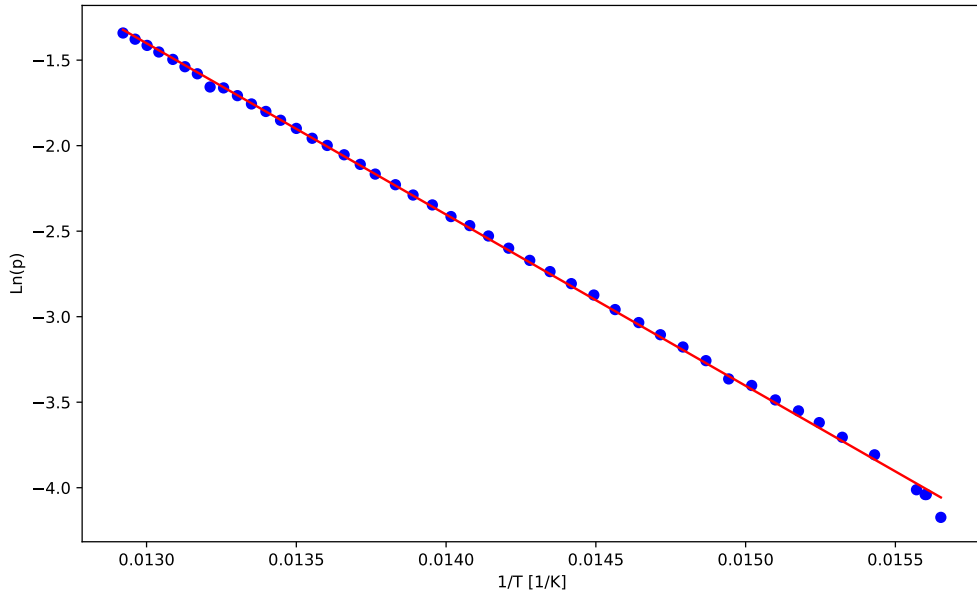


Figure 8: Plot of the logarithm of the pressure of argon in bar over  $\frac{1}{T}$ .

The resulting fit shows a straight line with the function  $y = m \cdot x + b$  with  $m = -1001.4 \text{ K}$  and  $b = 11.616$ . By using the equation

$$\Delta H_{\text{sub}} = m \cdot R,$$

the sublimation enthalpy of argon can be calculated as  $8325.640 \frac{\text{J}}{\text{mol}}$ .

By using equation 5 the inner energy of argon can be calculated.

$$\begin{aligned} U_s &= \frac{5}{2}RT - \Delta H_{\text{sub}} \\ &= \frac{5}{2} \cdot 8.314 \frac{\text{J}}{\text{mol} \cdot \text{K}} \cdot 70 \text{ K} - 8325.640 \frac{\text{J}}{\text{mol}} \\ &= -6870.69 \frac{\text{J}}{\text{mol}} \end{aligned}$$

As equation 6 shows, the lattice energy can be calculated with the internal energy and the vibrational energy. Therefore the vibrational energy has to be calculated, which can be done by using equation 7. The Debye temperature  $\Theta_D = 85 \text{ K}$  and the Debye funktion  $D\left(\frac{\Theta}{T}\right) = 0.617$  at  $70 \text{ K}$  are given, which means the vibrational energy can be

calculated as

$$\begin{aligned}
 U_{\text{vib}} &= \frac{9}{8} R \Theta_D + 3RTD \left( \frac{\Theta_D}{T} \right) \\
 &= \frac{9}{8} \cdot 8.314 \frac{\text{J}}{\text{mol} \cdot \text{K}} \cdot 85 \text{ K} + 3 \cdot 8.314 \frac{\text{J}}{\text{mol} \cdot \text{K}} \cdot 70 \text{ K} \cdot 0.617 \\
 &= 1872.271 \frac{\text{J}}{\text{mol}}
 \end{aligned}$$

The lattice energy can now be calculated by rearranging equation 6.

$$\begin{aligned}
 U_{\text{lattice,D}} &= U_s - U_{\text{vib}} \\
 &= -6870.69 \frac{\text{J}}{\text{mol}} - 1872.271 \frac{\text{J}}{\text{mol}} \\
 &= -8742.961 \frac{\text{J}}{\text{mol}}
 \end{aligned}$$

An alternative method of calculating the lattice energy is by using equation 8. To do this, the minimal distance  $a$  between atoms has to be calculated by using the equation for a face-centered cubic lattice and the lattice constant of argon which is given as  $5.43 \times 10^{-10} \text{ m}$ .

$$\begin{aligned}
 a &= \frac{1}{\sqrt{2}} \cdot 5.43 \times 10^{-10} \text{ m} \\
 &= 3.78 \times 10^{-10} \text{ m}
 \end{aligned}$$

With  $\sigma_0$  for argon given as  $3.41 \times 10^{-10} \text{ m}$  and  $\epsilon_0$  from the lennard-jones potential given as  $1.643 \times 10^{-21} \text{ J}$  the lattice energy can now be calculated.<sup>[2]</sup>

$$\begin{aligned}
 U_{\text{lattice,E}}(s) &= 2N_A \epsilon_0 \left[ 12.132 \left( \frac{\sigma_0}{a} \right)^{12} - 14.454 \left( \frac{\sigma_0}{a} \right)^6 \right] \\
 &= 2 \cdot 6.022 \times 10^{23} \frac{1}{\text{mol}} \cdot 1.643 \times 10^{-21} \text{ J} \\
 &\cdot \left[ 12.132 \cdot \left( \frac{3.41 \times 10^{-10} \text{ m}}{3.78 \times 10^{-10} \text{ m}} \right)^{12} - 14.454 \cdot \left( \frac{3.41 \times 10^{-10} \text{ m}}{3.78 \times 10^{-10} \text{ m}} \right)^6 \right] \\
 &= -8441.849 \frac{\text{J}}{\text{mol}}
 \end{aligned}$$

In comparison, the calculated lattice energies have a deviation of approximately 3.6%. This deviation can be explained by leaks in the measuring setup due to it not being perfectly isolated.

## 5 Error Discussion

## 6 Conclusion

The isochor simulation showed a similar sublimation curve as the experimental sublimation curve, but was located around 10K lower due to not enough iteration steps and cycles in the Velocity-Verlet algorithm and the approximations made in the used LJ-potential.

The three Isobaric simulation showed the importancy of of computational accuracy leading to a curve / value much more compareable to real, experimental data. Although even the simulation with the most computational accuracy showed a strong deviation to the measured value.

## 7 References

- [1] H. Dilger, *2025-pc2-script-en*, **2025**.
- [2] J. O. Hirschfelder, C. F. Curtiss, R. B. Bird, *The molecular theory of gases and liquids*, John Wiley & Sons, **1964**.
- [3] .